



An optimal selection method for debris flow scene symbols considering public cognition differences

Weilian Li ^{a,b}, Jun Zhu ^{b,*}, Yuhang Gong ^c, Qing Zhu ^b, Bingli Xu ^d, Min Chen ^b

^a Institute for Geodesy and Geoinformation, University of Bonn, Bonn, Germany

^b Faculty of Geosciences and Environmental Engineering, Southwest Jiaotong University, Chengdu, China

^c Sichuan Institute of Land Science and Technology (Sichuan Center of Satellite Application Technology), Department of Natural Resources of Sichuan Province, Chengdu, China

^d Department of Information and Communication Engineering, Academy of Army Armored Forces, Beijing, China

ARTICLE INFO

Keywords:

Debris flow scene symbol

Optimal selection

Public cognition

FAHP

3D visualization

ABSTRACT

Disaster scene symbols can reduce memory and cognitive burdens and improve the transmission efficiency of debris flow information. There is no unified standard for disaster scene symbols, although many academic institutions and emergency departments have thoroughly studied debris flow disasters. Instead, many disaster scene symbols of different styles interfere with the public's understanding of disaster information. Here, an optimal selection method for debris flow scene symbols considering public cognition differences is proposed. First, public knowledge is incorporated into the fuzzy analytic hierarchy process (FAHP) model for debris flow scene symbols selection. Second, debris flows are visualized in 3D with a virtual geographic environment (VGE). Finally, a real debris flow is selected for experimental analysis. The proposed method can support the optimal selection of debris flow scene symbols considering public cognition differences, and a 3D scene constructed with the selected scene symbols can improve the transmission efficiency of disaster information and provide support for public-oriented debris flow information services.

1. Introduction

Debris flow is a common and frequent type of geological disaster that is sudden and involves severe destruction and a short response time [1–3]. Because of the specific topography and climatic conditions in the mountainous area of Southwest China, debris flows have recently occurred every rainy season, which seriously threatens lives and property [4–7]. Traditional structural measures play a very important role in debris flow prevention and mitigation. However, disasters will always occur, the core idea of debris flow mitigation should transform from “disaster control” to “disaster management” [8–11]. The general public is most deeply affected by debris flow disasters, and strengthening the risk awareness and self-adjustment ability of the public is an important part of disaster management and an effective means to reduce disaster losses [12,13].

As an effective type of nonstructural measure, a disaster map is the product of interdisciplinary knowledge integration and a powerful tool to help people understand disaster risks and increase disaster reduction awareness [14–17]. Moreover, the development of 3D geographic information system (GIS) and virtual geographic environment (VGE) compensates for the deficiency of accuracy, expressiveness, and intuitiveness in 2D disaster maps and supports users in scanning disaster information in a comprehensive way that is close to reality [18–25]. Symbols are important carriers in disseminating disaster information regardless of whether disaster maps or

* Corresponding author.

E-mail address: zhujun@swjtu.edu.cn (J. Zhu).

3D disaster scenes are used. A disaster scene symbol is a kind of graphic symbol with visual and spatial characteristics that can represent the spatial location, influence range, and evolution trend of debris flow disasters [15,26–28].

The self-explanatory nature of disaster scene symbols can enhance the dissemination efficiency of disaster information and reduce the memory and cognitive burden of the public, thereby enhancing the public's awareness and understanding of debris flow disasters [29–31]. At present, academic institutions and emergency departments each have their own disaster scene symbol standards. For example, the Federal Geographic Data Committee (FGDC) of the United States has proposed a set of systematic disaster scene symbol standards, and the content covers almost all-natural and man-made disasters [32,33]. Canada has proposed the Canadian All Hazards Symbology to meet the needs of government operation centers for disaster management [34]. The Emergency Management Spatial Information Network Australia (EMSINA) also proposed a set of Australian All Hazards Symbology, which is the standard symbology used in map products provided by the Australian emergency management agency [35]. The Chinese government also proposed a national standard specification for emergency response plotting symbols [36]. Many effective studies have been carried out on disaster scene symbols, and we have strong reason to believe that these symbols are designed for the same purpose. However, the existence of different types of disaster scene symbols greatly interferes with the public's cognition of disaster information due to objective semantic deviations. In addition, different members of the public have a different understanding of and requirements for debris flow scene symbols due to differences in knowledge structures, so it is necessary to explore the laws of public cognition concerning debris flow scene symbols and to select a set of scene symbols with the highest dissemination efficiency for disaster information, taking into account differences in public cognition.

In this paper, we propose an optimal selection method for debris flow scene symbols considering public cognition differences. The aim is to consider the public cognition differences in the process of selecting debris flow scene symbols, to obtain a set of scene symbols with high dissemination efficiency for disaster information. Based on the optimized symbol sets, 3D scenes of debris flows are constructed to provide disaster information services for the public. We mainly focus on the construction of a fuzzy analytic hierarchy process (FAHP) model for the optimal selection of debris flow scene symbols and 3D visualization integrated with the VGE. The remainder of this paper is organized as follows: Section 2.1 introduces the overall research framework of this paper. Section 2.2 provides the core idea of the optimal selection of debris flow scene symbols. Section 2.3 introduces the 3D visualization of debris flows integrated with the VGE. Section 3 describes the experiment analysis. Section 4 presents the conclusion and future work.

2. Methodology

2.1. Overall research framework

Fig. 1 shows the overall research framework of this paper, which includes disaster scene symbol set, optimal selection, and 3D visualization of debris flow. First, the disaster scene symbol set is obtained based on relevant global or local standards and literature. Second, a FAHP model for optimal selection of debris flow scene symbols is constructed. Finally, based on the optimized set of debris flow scene symbols and disaster datasets, 3D visualization of debris flow disasters is realized.

2.2. Optimal selection of debris flow scene symbols

Optimal selection is described in this paper as the selection of a set of debris flow scene symbols from different symbol standards that are preferred and appropriate by the public according to their cognitive differences, thus providing a basis for public-oriented 3D virtual scenes construction. This paper adopts the FAHP and considers public cognition differences in selecting debris flow scene symbols. The FAHP is a qualitative and quantitative analysis method that combines the analytic hierarchy process and fuzzy comprehensive evaluation [37,38]. The FAHP can integrate and quantify the public's cognitive differences and needs to perform the optimal selection of debris flow scene symbols.

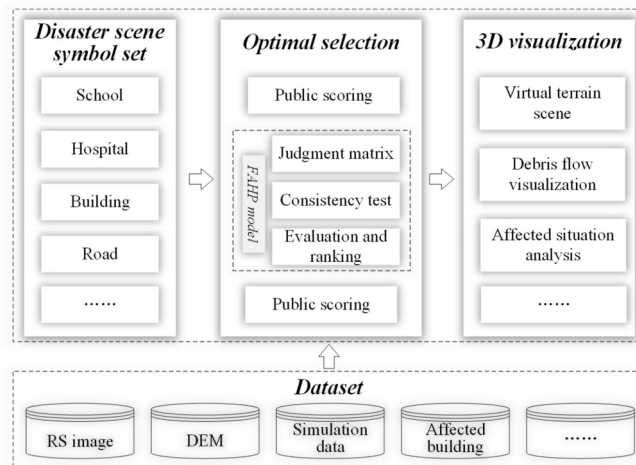


Fig. 1. Overall research framework.

The algorithm flow is shown in Fig. 2. First, the rules and sublevel indices for the optimal selection of debris flow scene symbols are determined. Second, public cognition differences are incorporated into the judgment matrix. Third, the sort weight vector of the judgment matrix is determined. Finally, based on a Likert scale, the comprehensive score of each disaster scene symbol is obtained by multiplying the public score and the total ranking weight, and then the optimized set of debris flow scene symbols is determined [39].

For the flow chart, it is necessary to further explain the public, disaster scene symbol set, and Likert scale.

The participating public should be an opportunistic sample involving no particular section of the population, the number of the respondents is determined by reference to Taherdoost [40]. To reflect the randomness and universality of the sample, this paper plan to adopt an online anonymous survey to collect the public cognition feedback, and some basic information such as gender, age, and education level of the participants should be recorded. Respondents' ages are divided into 4 intervals (under 18, 18–29, 30–39, and over 40), and their education degrees mainly include middle school, high school, undergraduate, and master or higher.

The disaster scene symbol set is the basis for public cognition. It is formed mainly with reference to some global or local standards for disaster scene symbols, such as Emergency and Hazards Mapping Symbology (EHMS) proposed by the Federal Emergency Management Agency (FEMA), Canadian All-Hazards Symbology (CAHS) proposed by Government Operation Centers (GOC), Australian All Hazards Symbology (AAHS) proposed by Australian Emergency Management Agency (AEMA), European Emergency 2D/3D Symbology and so on. Moreover, some knowledge of expert research and literature review are also incorporated into the disaster scene symbol set establishment.

The Likert scale is the most popular rating scale of attitudes, beliefs, and opinions (a 5-point scale, with 5 being the highest rating) [39]. The advantageous side of the Likert scale is that they are the most universal method for survey collection, therefore they are easily understood. It does not require respondents to provide simple and specific yes or no answers, which somewhat reduces the subjectivity of the respondents and makes it easier for them to answer the questions. Likert scale surveys are also quick, efficient, and inexpensive methods for data collection, they are highly versatile and can be sent via mail, the internet, or in person. Therefore, the Likert scale applies to public surveys with different locations and different knowledge backgrounds.

2.2.1. FAHP model for the optimal selection of debris flow scene symbols

A disaster scene symbol is a tool for debris flow information transmission, communication, and thinking, which can provoke subjective responses from the public and effectively compensate for the lack of expressiveness of natural language at the geographic space level. The efficiency and effectiveness of disaster information transmission are the key factors to be considered in the selection of debris flow scene symbols. In this paper, we divide the target layer into three rule layers based on expressiveness, semanticity, and functionality, and twelve subindices are subdivided under the rule layers, as shown in Fig. 3.

- (1) Expressiveness is a rule for determining the selection of debris flow scene symbols from a design perspective. This element reflects the basic characteristics of disaster scene symbols, including clarity, conciseness, intuitiveness, and artistry.
- (2) Semanticity analyzes the efficiency and effectiveness of disaster scene symbols in transmitting disaster information from the perspective of information dissemination. The self-explanatory nature of disaster scene symbols can elicit users' mental associations and form short-term memories to improve the understanding of debris flows.

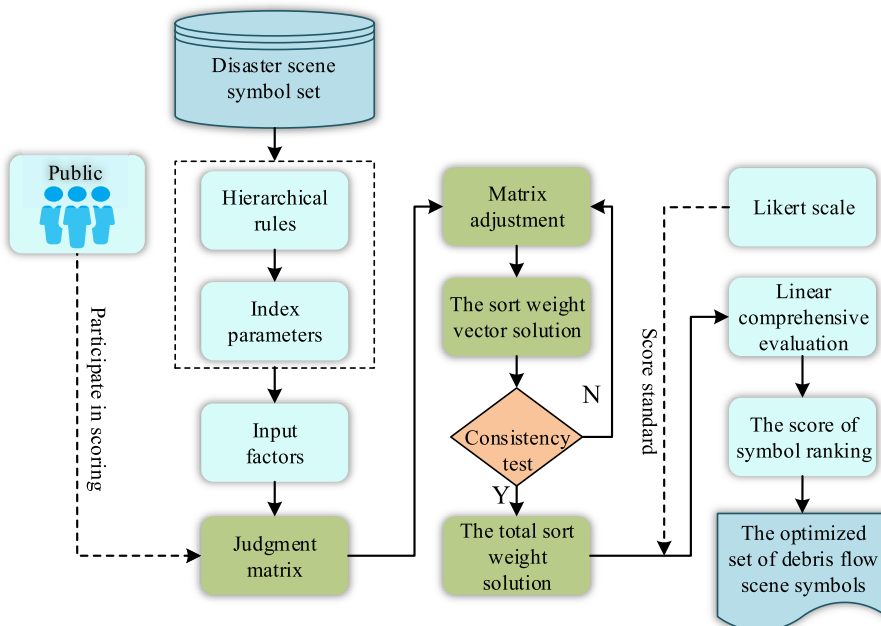


Fig. 2. Algorithm flow of the optimal selection of debris flow scene symbols.

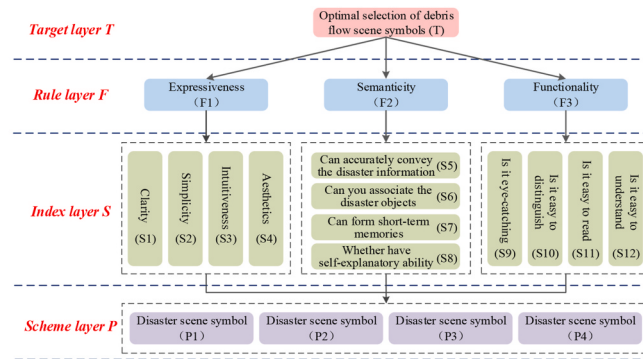


Fig. 3. The hierarchical structure of the optimal selection of debris flow scene symbols.

(3) Functionality: Disaster scene symbols not only need to be expressive but also need to have functional value. Functionality analyzes whether disaster scene symbols can be quickly and accurately recognized by users from the perspective of spatial cognition.

2.2.2. Judgment matrix and index weight

(1) The construction of the judgment matrix

The factors that affect the selection of debris flow scene symbols include F1, F2, F3, S1, S2, ..., and S12. These factors can be compared in pairs by referring to a 0.1–0.9 scale, as shown in Table 1.

Therefore, the fuzzy judgment matrix $A = (a_{ij})_{n \times n}$ can be obtained, where $0 \leq a_{ij} \leq 1, (i, j = 1, 2, \dots, n)$, and the fuzzy matrix A meets the following conditions:

- ① if $i = j$, $a_{ij} = 0.5$;
- ② $a_{ij} + a_{ji} = 1$.

(2) Single-sort weight calculation

We suppose that there are n first-level indices in rule layer F and that the corresponding weight vector is $W = [w_1^A, w_2^A, \dots, w_n^A]$; then, the single-sort weight of the rule level can be calculated by formula 1.

$$w_i^A = \frac{1}{n} - \frac{1}{2\alpha} - \frac{\sum_{k=1}^n a_{ik}}{n\alpha}, i \in (1, 2, \dots, n) \quad (1)$$

where α is the factor that measures the difference between rule levels ($w_i^A - w_j^A$). Generally, the smaller the α value is, the more closely the experts pay attention to the difference in the importance of the various rules during the construction of the judgment matrix [41]. In actual calculations, generally, $\alpha = (n-1)/2$.

If the i th rule contains m indices, it is expressed as b_1, b_2, \dots, b_m , and the single-sort weight of the index level can be obtained (formula 2).

$$w_{ij}^B = \frac{1}{m} - \frac{1}{2\beta} - \frac{\sum_{k=1}^m b_{ik}}{m\beta}, i \in (1, 2, \dots, m) \quad (2)$$

where β is the factor that measures the difference between rule levels ($w_{ii}^B - w_{jj}^B$). In actual calculations, generally, $\beta = (m-1)/2$.

(3) Consistency test

Then, the fuzzy consistency test is adopted to verify the rationality of the fuzzy judgment matrix. Let $w_{ij}^* = \frac{w_i^A}{w_i^A + w_j^A}, (i, j = 1, 2, \dots, n)$;

Table 1

Description of the 0.1–0.9 importance scale.

Scale	Description
0.5	The two factors are of equal importance
0.6	One factor is slightly more important than the other
0.7	One factor is obviously more important than the other
0.8	One factor is more important than the other
0.9	One factor is much more important than the other
0.1, 0.2, 0.3,	Inverse comparison; if the factor a_i is compared with the factor a_j to obtain the scale value a_{ij} , then the scale value of the factor a_j compared with the factor a_i is $1-a_{ij}$. For example, if the factor a_1 is compared with the factor a_2 to obtain the scale value $a_{12} = 0.3$, then in turn $a_{21} = 0.7$
0.4	

then, the characteristic matrix of matrix A can be obtained as shown in formula (3):

$$W^* = \left(w_{ij}^* \right)_{n \times n}^A \quad (3)$$

The compatibility index I is adopted to test the consistency of the judgment matrix and the characteristic matrix. The calculation method is shown in formula (4):

$$I(A, W^*) = \frac{1}{n^2} \sum_{i=1}^n \sum_{j=1}^n |a_{ij} + w_{ji}^* - 1| \quad (4)$$

If $I(A, W^*) < \delta$, the consistency of the fuzzy judgment matrix is high, and δ indicates the tolerance of the public for the consistency test of the judgment matrix. The smaller the value is, the higher the requirement for the consistency of the judgment matrix. In this paper, we set $\delta = 0.1$ [42].

(4) Whole-sort weight calculation

If all the fuzzy judgment matrices pass the consistency test, then the whole-sort weight vector of each index corresponding to the target layer T is $W_T = [w_{T_1}, w_{T_2}, \dots, w_{T_n}]$, and the calculation method is shown in formula (5):

$$w_{T_i} = \sum_{i=1}^n w_i^A w_{ij}^B \quad (5)$$

2.2.3. Comprehensive evaluation of the debris flow scene symbol selection scheme

The weight value of each factor that affects the selection of the debris flow scene symbols can be obtained based on the FAHP. Then, we refer to a Likert scale to allow the public to score each symbol according to the indices. Finally, a linear comprehensive evaluation method is used to construct a comprehensive evaluation model for the optimal selection of debris flow scene symbols, as shown in formula (6):

$$S = \sum_{i=1}^n w_{T_i} \times x_i \quad (6)$$

In this formula, S indicates the total scores of different disaster scene symbols, w_{T_i} indicates the total consistency weight of each index, and x_i represents the public's score for each index.

2.3. The 3D visualization of debris flow integrated with the VGE

The VGE is constructed based on spatial data and geographic models, which can realize a multi-dimensional, multi-viewpoint, and multi-detail visual representation of the real world [43,44]. Debris flow visualization integrated with the VGE can yield a fusion representation and enable sharing of disaster information and knowledge. The workflow of debris flow 3D visualization is shown in Fig. 4. It includes the following three main parts:

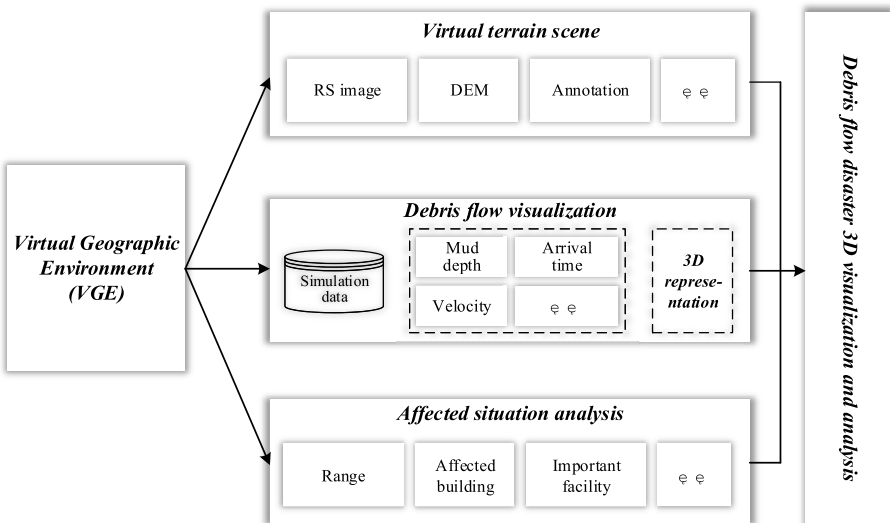


Fig. 4. 3D visualization method of the debris flow disaster process.

- (1) Virtual 3D terrain scene: The terrain scene is the basis for debris flow visualization. High-resolution remote sensing image data and digital elevation model (DEM) data can be used to construct a terrain scene. The remote sensing image is mapped to the terrain as a texture, which can greatly enhance the realism of the 3D scene.
- (2) Spatiotemporal process of debris flow visualization: The simulation data of a debris flow include mud depth, flow velocity, and arrival time. The state value of the grid is dynamically changed through continuous-time changes; a one-to-one mapping and a continuous-color ribbon are used to show the mud depth value at each moment; and the arrival time, inundated area, and flow velocity are represented simultaneously.
- (3) Representation and analysis of disaster results: Disaster results are often more important than their spatiotemporal process in the dissemination of disaster information. Therefore, disaster information such as that of the roads, buildings, and infrastructures affected by debris flows are symbolized in the 3D scene to improve the transmission efficiency of risk information.

3. Experiment analysis

3.1. Description of the experiment data

In this paper, the debris flow that occurred in Shuimo town, Wenchuan County, Sichuan Province ($30^{\circ}55'N$ $103^{\circ}22'E$ ~ $103^{\circ}25'E$), was selected as the case area to carry out the experimental analysis. We referred to international standards such as ANSI, CAHS, EHMS, and AAHS and some relevant literature to collect debris flow scene symbols [30,32–35]. These symbols have different styles and abilities to convey information, as shown in Fig. 5. Moreover, high-resolution images with a resolution of 0.5 m and DEM data with a resolution of 10 m were also collected, and thematic data and debris flow simulation data were provided by Yin et al. [45].

3.2. Index weight value integrated with public perception

To incorporate public knowledge into the construction of the judgment matrix for the optimal selection of debris flow scene symbols, we chose to issue questionnaires to the public online. The public referred to the 0.1–0.9 scale to compare and score the indices. A total of 174 questionnaires were collected, and 165 questionnaires were considered valid after excluding invalid and repeated questionnaires. The validity test results of this questionnaire are shown in Table 2.

The reliability (α) and validity (KMO) values of this questionnaire were both within the interval (0.7–0.8), and Bartlett's test reached an extremely significant level. This comprehensively proves that the reliability and validity of these questionnaires are of high quality [46,47]. The results of the questionnaire can be further analyzed. The reason why the reliability and validity of the questionnaire are not higher than 0.8 is that there was a large difference in public knowledge structures, and it was difficult to ensure that all members of the public achieved a consistent understanding of each index of the questionnaire. Therefore, to allow for different levels of knowledge among members of the public, the questionnaire should use simple words instead of technical terms to prevent the survey results from being affected by the influence of unfamiliar terminology [48]. The expected public knowledge for the debris flow-related disaster mitigation should include knowing what a debris flow is, what factors cause it, and what devastating consequences it can have [6,49,50]. On this basis, disaster education can help the public to further understand disaster prevention measures and improve their risk awareness. Fig. 6 shows the statistical results of the questionnaire. This paper uses the median and standard deviation to analyze the results of the users' evaluations of index importance. The median reflects the central trend of user feedback, and the standard deviation represents the degree of dispersion and the stability of the preset questionnaire.

As shown in Fig. 6(c), in terms of semanticity, the results of S6–S5 ($M = 0.3$, $SD = 0.13$), S7–S5 ($M = 0.3$, $SD = 0.16$), S8–S5 ($M = 0.4$, $SD = 0.16$), S7–S6 ($M = 0.4$, $SD = 0.15$), S8–S6 ($M = 0.5$, $SD = 0.19$), and S8–S7 ($M = 0.6$, $SD = 0.17$) represent that most people believe that the self-explanatory nature of disaster scene symbols and the ability to accurately convey disaster information are the key factors. As shown in Fig. 6(d), in terms of functionality, the results of S10–S9 ($M = 0.5$, $SD = 0.17$), S11–S9 ($M = 0.6$, $SD = 0.17$), S12–S9 ($M = 0.7$, $SD = 0.17$), S11–S10 ($M = 0.6$, $SD = 0.18$), S12–S10 ($M = 0.7$, $SD = 0.18$), and S12–S11 ($M = 0.7$, $SD = 0.17$) show that the most important function of disaster scene symbols for the public is that they are easy to read, and the importance of this factor is obviously greater than that of other functional indicators.

Through the above analysis, we can construct the first-level rule judgment matrix F and the sublevel index judgment matrices F1~F3:

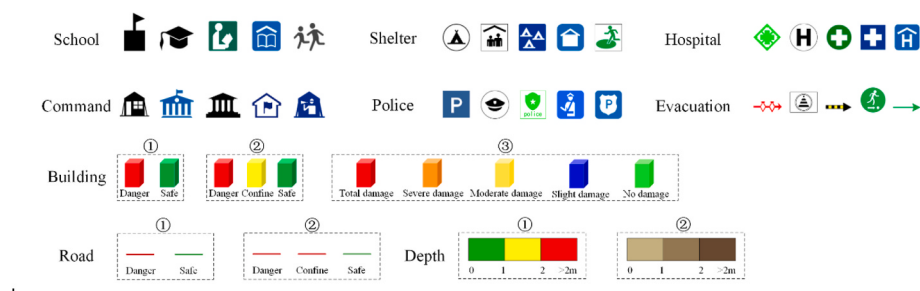
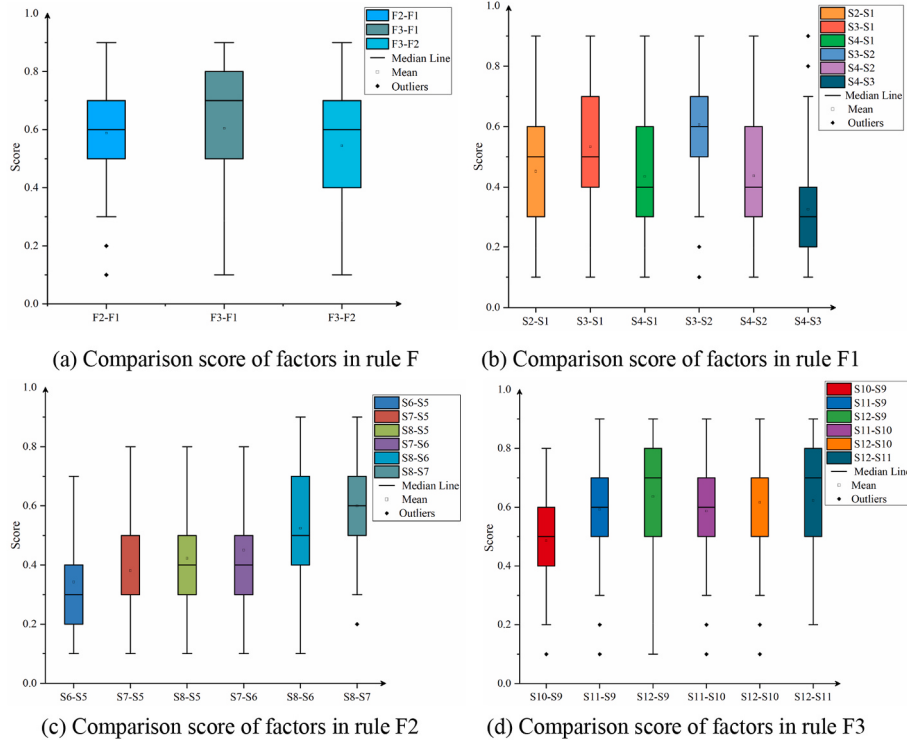


Fig. 5. Alternatives of debris flow scene symbols.

Table 2

Reliability and validity test results.

Cronbach's α for reliability	KMO for Validity	Bartlett's test for Significance		
		Approx. chi-square	df	Sig.
0.746	0.730	751.793	210	0.000** < 0.01

**Fig. 6.** Statistical analysis of the questionnaire for the factor comparison.

As shown in Fig. 6(a), the results of F2-F1 ($M = 0.60$, $SD = 0.21$), F3-F1 ($M = 0.7$, $SD = 0.20$)), and F3-F2 ($M = 0.60$, $SD = 0.20$) show that most people believe that the semanticity of debris flow scene symbols is slightly more important than expressiveness, functionality is obviously more important than expressiveness, and functionality is slightly more important than semanticity. As shown in Fig. 6(b), in terms of the expressiveness of disaster scene symbols, the results of S2-S1 ($M = 0.50$, $SD = 0.19$), S3-S1 ($M = 0.50$, $SD = 0.19$), S4-S1 ($M = 0.40$, $SD = 0.20$), S3-S2 ($M = 0.6$, $SD = 0.18$), S4-S2 ($M = 0.4$, $SD = 0.20$), and S4-S3 ($M = 0.3$, $SD = 0.14$) indicate that most people think clarity is as important as simplicity and intuitiveness, clarity is slightly more important than aesthetics, intuitiveness is slightly more important than simplicity, simplicity is slightly more important than aesthetics, and intuitiveness is obviously more important than aesthetics.

$$F = \begin{bmatrix} 0.5 & 0.4 & 0.3 \\ 0.6 & 0.5 & 0.4 \\ 0.7 & 0.6 & 0.5 \end{bmatrix} \quad (7)$$

$$F_1 = \begin{bmatrix} 0.5 & 0.5 & 0.5 & 0.6 \\ 0.5 & 0.5 & 0.4 & 0.6 \\ 0.5 & 0.6 & 0.5 & 0.7 \\ 0.4 & 0.4 & 0.3 & 0.5 \end{bmatrix} \quad (8)$$

$$F_2 = \begin{bmatrix} 0.5 & 0.7 & 0.7 & 0.6 \\ 0.3 & 0.5 & 0.6 & 0.6 \\ 0.3 & 0.4 & 0.5 & 0.4 \\ 0.4 & 0.5 & 0.6 & 0.5 \end{bmatrix} \quad (9)$$

$$F_3 = \begin{bmatrix} 0.5 & 0.5 & 0.4 & 0.3 \\ 0.5 & 0.5 & 0.4 & 0.3 \\ 0.6 & 0.6 & 0.5 & 0.3 \\ 0.7 & 0.7 & 0.7 & 0.5 \end{bmatrix} \quad (10)$$

On this basis, the F layer can be solved by single sorting to obtain the weight value of the rule layer: $W = [0.23, 0.33, 0.44]$; the compatibility index $I(F, W^*)$ equals 0.018, less than 0.1, which indicates that rule layer F's judgment matrix passes the consistency test. At the same time, the weight value of each index can be calculated $W_1 = [0.27, 0.25, 0.3, 0.18]$, $W_2 = [0.33, 0.25, 0.18, 0.24]$, and $W_3 = [0.20, 0.20, 0.25, 0.35]$, and the compatibility indicators are 0.025, 0.043, and 0.048, respectively, all less than 0.1. The total ranking weight vector of the index layer can be calculated as shown in Table 3. The most important index is whether the disaster scene symbols are easy to read, followed by whether they are easy to distinguish and then whether they can accurately transmit disaster information and whether they are self-explanatory.

3.3. The final scores of the debris flow scene symbols in different indices

In addition, this paper randomly selected 30 persons and collected the scores of the disaster scene symbols under each index. The score results are shown in Fig. 7.

The statistical results show that the average score of school symbol 2 in most indices is higher than those of the other school symbols; the reason is that this symbol has a strong explanatory ability with the mortarboard hat as the background that is not affected by language or cultural differences. However, it is not very friendly to the less educated public. The mean score of shelter symbol 2 in most indices is higher than those of other shelter symbols because the combination of the schematic roof and the victims can intuitively convey the information of a shelter. Since the main bodies of hospital symbols 3 and 4 are both "+", their mean scores are very close, and this symbol conforms to public perceptions of hospitals fairly well. Although the letter H is also a common symbol of hospitals, it is affected by language and cultural differences.

Typically, members of the general public, especially those who have not personally experienced a disaster, have little contact with emergency command centers. Therefore, the public's perception of the abovementioned five types of emergency command symbols is quite variable, and none of the symbols absolutely conforms to the public's perception. However, the overall score of symbol 5 is relatively high. Regarding the symbolic representation of affected buildings and roads, it can be concluded from the public feedback that these types of symbols are acceptable to the public, but they prefer that they be represented in a simple "binary" way; that is, they only need to know whether the symbols indicate danger or safety. Regarding mud depth, the public prefers to use gray for the visual display of debris flows. The reason is that gray is more in line with the public's cognition of debris flows, while red, yellow, and green emergency color bands are more suitable for experts in conducting disaster risk assessment and display.

Based on the weight of each index and the scores of the symbols under each index, the final score of each debris flow scene symbol can be calculated, as shown in Table 4.

Through the above comprehensive analysis, it can be concluded that the set of debris flow scene symbols that match public cognition is as shown in Fig. 8.

3.4. The 3D visualization of debris flow disasters

Based on the abovementioned optimized set of debris flow scene symbols, we use HTML5, JavaScript, CSS3, and the 3D open-source library Cesium.js to obtain a dynamic visualization of debris flow disasters in a network environment. Disaster scene symbols are adopted to represent the spatial distribution and accessibility of some important infrastructures, such as affected buildings, affected roads, schools, and hospitals, as shown in Fig. 9. The combination of the internet, 3D visualization, and disaster scene symbols can provide debris flow information services to people in different locations, promote their understanding of debris flows, and ultimately achieve the goal of enhancing their risk awareness.

4. Conclusion and future work

Debris flow scene symbols can enhance the efficiency of disseminating disaster information and reduce the public's cognitive burden. However, different agencies and institutions have their own disaster scene symbol standards. These symbols are designed with expert knowledge as the guide. Employing various disaster scene symbols not only makes it difficult to improve the dissemination efficiency of debris flow information but also leads to cognitive differences in the public. Therefore, based on existing debris flow scene symbols, this paper determined the public's cognitive differences regarding different symbols, combined these differences with the FAHP model to perform the optimal selection of debris flow scene symbols, and yielded a set of debris flow scene symbols considering public perception needs. Next, the main contribution of this paper is summarized.

Table 3
Final weight values of index layers.

W_T	W_{S_1}	W_{S_2}	W_{S_3}	W_{S_4}	W_{S_5}	W_{S_6}
Value	0.0621	0.0575	0.069	0.0414	0.1089	0.0825
W_T	W_{S_7}	W_{S_8}	W_{S_9}	$W_{S_{10}}$	$W_{S_{11}}$	$W_{S_{12}}$
Value	0.0594	0.1056	0.088	0.088	0.110	0.154

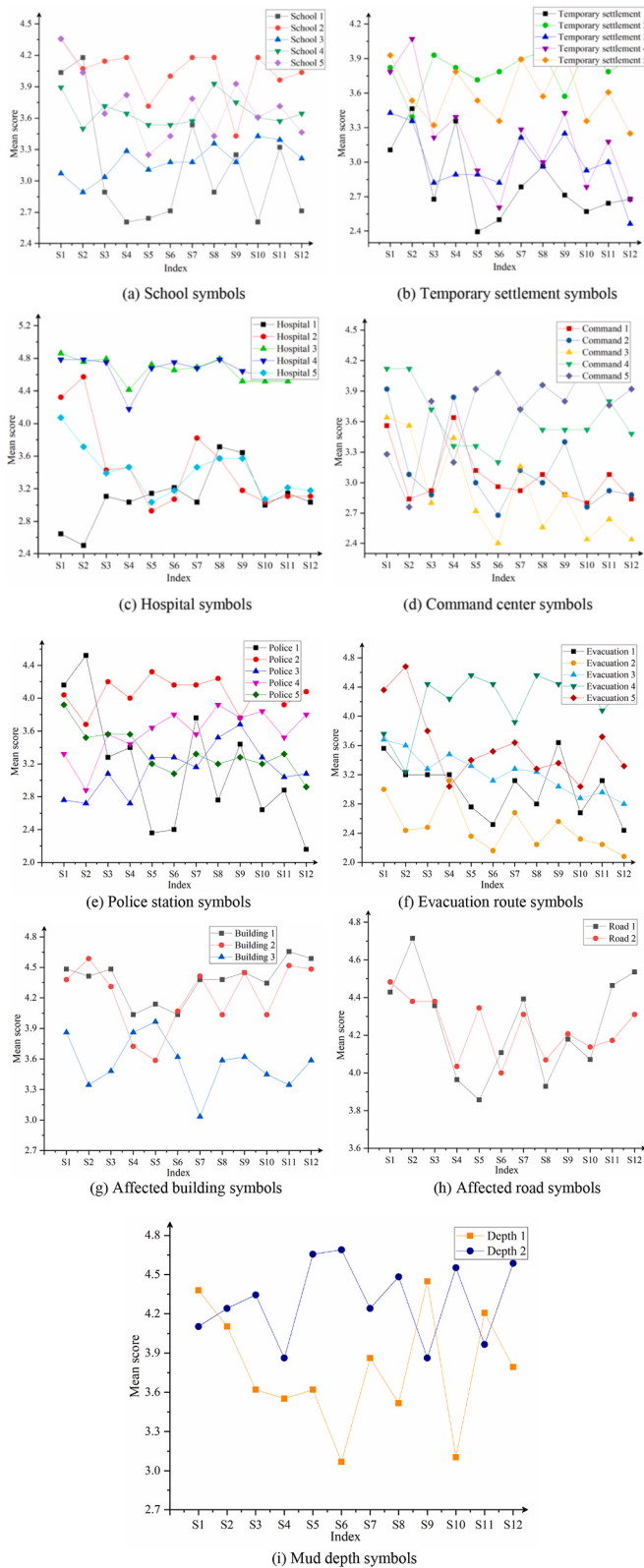
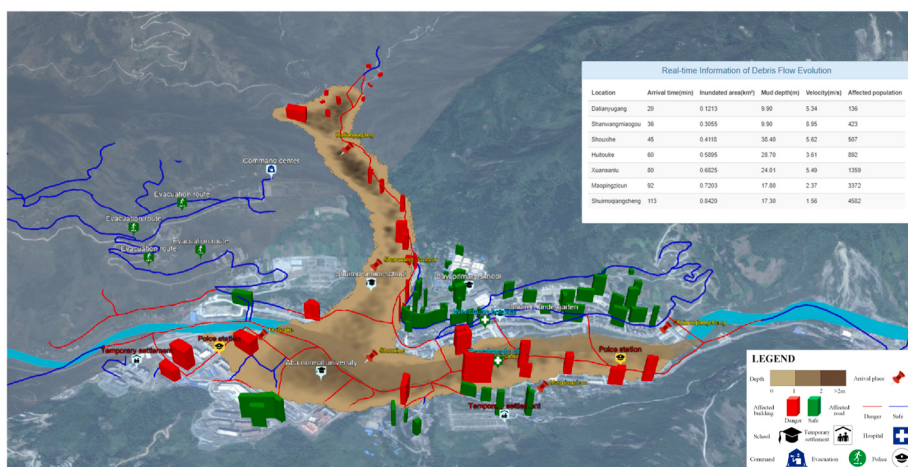


Fig. 7. Statistical analysis of debris flow scene symbol scores.

Table 4

Final scores of the debris flow scene symbols.

Symbol	Total score	Symbol	Total score	Symbol	Total score
School 1	3.12	Temporary settlement 1	2.83	Hospital 1	3.23
School 2	4.11	Temporary settlement 2	3.91	Hospital 2	3.45
School 3	3.30	Temporary settlement 3	3.03	Hospital 3	4.79
School 4	3.76	Temporary settlement 4	3.19	Hospital 4	4.84
School 5	3.74	Temporary settlement 5	3.64	Hospital 5	3.45
Command 1	3.10	Police 1	3.04	Evacuation 1	3.02
Command 2	3.13	Police 2	4.19	Evacuation 2	2.45
Command 3	2.85	Police 3	3.26	Evacuation 3	3.24
Command 4	3.68	Police 4	3.74	Evacuation 4	4.39
Command 5	3.88	Police 5	3.36	Evacuation 5	3.63
Building 1	4.51	Road 1	4.36	Depth 1	3.86
Building 2	4.33	Road 2	4.34	Depth 2	4.46
Building 3	3.66				

**Fig. 8.** A set of debris flow scene symbols that match public perception.**Fig. 9.** The 3D visualization of a debris flow integrated with the VGE.

First, a FAHP model for the optimal selection of debris flow scene symbols was designed, and the factors that affect the public's selection of debris flow scene symbols were determined. The rule layer mainly includes expressiveness, semanticity, and functionality, and each rule contains 4 secondary indices. Second, the public made a pairwise comparison of the impact factors and scored each symbol based on a Likert scale. Public participation can avoid the subjective effects of experts to a certain extent. The comprehensive score of each symbol was calculated to determine a set of debris flow scene symbols, and this set of symbols reflects the public perception preferences. Finally, the 3D visualization of a debris flow integrated with the VGE framework was realized, and the combination of the intuitive debris flow disaster representation and disaster scene symbols can meet the public's requirement for the true reproduction of debris flow processes while delivering semantic disaster information.

Although this paper incorporates the public perception difference into the selection of debris flow scene symbols, a set of scene symbols for debris flows that considers the public's perception preferences has been obtained, which can improve the public's cognitive efficiency to a certain extent. However, the optimal selection of disaster scene symbols does not incorporate public perception preferences into symbol design, so the public is still passive in accepting disaster information. In future works, eye tracking and virtual reality experiments can be considered in obtaining user perception information. This feedback can be used to optimize the design of debris flow scene symbols and ultimately achieve a two-way improvement in debris flow disaster information transmission and public awareness.

Declaration of competing interest

The authors declare that they have no known competing financial interests or personal relationships that could have appeared to influence the work reported in this paper.

Acknowledgments

This paper was supported by the National Natural Science Foundation of China (Grant Nos. U2034202, 41871289, and 41771442) and the Sichuan Science and Technology Program (Grant Nos. 2020JDTD0003, 2020YFG0083, and 2021088).

References

- [1] M. Jakob, Debris-flow hazard analysis, in: M. Jakob, O. Hungr (Eds.), *Debris-flow Hazards and Related Phenomena*, Praxis-Springer, Berlin, 2005, pp. 411–443.
- [2] P. Cui, Progress and prospects in research on mountain hazards in China, *Prog. Geogr.* 33 (2014) 145–152.
- [3] W.L. Li, J. Zhu, Y.H. Zhang, et al., A fusion visualization method for disaster information based on self-explanatory symbols and photorealistic scene cooperation, *ISPRS Int. J. Geo-Inf.* 8 (3) (2019), 104.
- [4] J. Huang, R. Huang, N. Ju, Q. Xu, C. He, 3D WebGIS-based platform for debris flow early warning: a case study, *Eng. Geol.* 197 (2015) 57–66.
- [5] C. Ouyang, K. Zhou, Q. Xu, et al., Dynamic analysis and numerical modeling of the 2015 catastrophic landslide of the construction waste landfill at Guangming, Shenzhen, China, *Landslides* 14 (2) (2017) 705–718.
- [6] W.L. Li, J. Zhu, L. Fu, et al., An augmented representation method of debris flow scenes to improve public perception, *Int. J. Geogr. Inf. Sci.* 35 (8) (2021) 1521–1544, <https://doi.org/10.1080/13658816.2020.1833016>.
- [7] D. Song, X. Chen, G.G.D. Zhou, et al., Impact dynamics of debris flow against rigid obstacle in laboratory experiments, *Eng. Geol.* 291 (2021), <https://doi.org/10.1016/j.enggeo.2021.106211>.
- [8] R.W. Perry, M.K. Lindell, Principles for managing community relocation as a hazard mitigation measure[J], *J. Contingencies Crisis Manag.* 5 (1) (1997) 49–59.
- [9] D.S. Mileti, *Design, D. A Reassessment of Natural Hazards in the United State*, Joseph Henry Press, Washington, DC, USA, 1999.
- [10] C.H. Sung, S.C. Liaw, A GIS-based approach for assessing social vulnerability to flood and debris flow hazards, *Int. J. Disaster Risk Reduct.* 46 (2020), <https://doi.org/10.1016/j.ijdrr.2020.101531>.
- [11] L. Zhou, X. Wu, Z. Xu, et al., Emergency decision making for natural disasters: an overview, *Int. J. Disaster Risk Reduct.* 27 (2018) 567–576.
- [12] Y. Ao, H. Zhang, L. Yang, Y. Wang, I. Martek, G. Wang, Impacts of earthquake knowledge and risk perception on earthquake preparedness of rural residents, *Nat. Hazards* 107 (2) (2021) 1287–1310.
- [13] Y. Ao, Y. Zhang, Y. Wang, Y. Chen, L. Yang, Influences of rural built environment on travel mode choice of rural residents: The case of rural Sichuan, *J Transport Geogr.* 85 (2020) 102708.
- [14] EXCIMAP, *Handbook on Good Practice for Flood Mapping in Europe*. European Exchange Circle on Flood Mapping, 2007.
- [15] K.A. Mamata, First responders and crisis map symbols: clarifying communication, *Cartogr. Geogr. Inf. Sci.* 36 (1) (2009) 19–28.
- [16] M.A.T. Clive, J.M. Lindsay, G.S. Leonard, et al., Volcanic hazard map visualization affects cognition and crisis decision-making, *Int. J. Disaster Risk Reduct.* 55 (2021), <https://doi.org/10.1016/j.ijdrr.2021.102102>.
- [17] C.C. MacPherson-Krutschy, B.D. Brand, M.K. Lindell, Does updating natural hazard maps to reflect best practices increase viewer comprehension of risk? *Int. J. Disaster Risk Reduct.* 46 (2020) <https://doi.org/10.1016/j.ijdrr.2020.101487>.
- [18] H. Lin, M. Chen, G.N. Lü, et al., Virtual geographic environments (VGEs): a new generation of geographic analysis tool, *Earth Sci. Rev.* 126 (2013) 74–84.
- [19] H. Lin, M. Chen, G.N. Lü, Virtual geographic environment: a workspace for computer-aided geographic experiments, *Ann. Assoc. Am. Geogr.* 103 (3) (2013) 465–482.
- [20] H. Lin, M. Chen, Managing and sharing geographic knowledge in virtual geographic environments (VGEs), *Spatial Sci.* 21 (4) (2015) 261–263.
- [21] F. Macchione, P. Costabile, C. Costanzo, et al., Moving to 3-D flood hazard maps for enhancing risk communication[J], *Environ. Model. Software* 111 (2019) 510–522.
- [22] M. Chen, H. Lin, Virtual geographic environments (VGEs): originating from or beyond virtual reality (VR)? *Int. J. Digital Earth* 11 (4) (2018) 329–333, <https://doi.org/10.1080/17538947.2017.1419452>.
- [23] M. Chen, et al., Position paper: open web-distributed integrated geographic modelling to enable wider participation and model application, *Earth Sci. Rev.* 207 (2020), 103223, <https://doi.org/10.1016/j.earscirev.2020.103223>.
- [24] G.N. Lü, et al., Reflections and speculations on the progress in Geographic Information Systems (GIS): a geographic perspective, *Int. J. Geogr. Inf. Sci.* 33 (2) (2019) 346–367, <https://doi.org/10.1080/13658816.2018.1533136>.
- [25] Y. Li, J.H. Gong, H. Liu, et al., Real-time flood simulations using CA model driven by dynamic observation data, *Int. J. Geogr. Inf. Sci.* 29 (4) (2015) 523–535.
- [26] M. Konecny, T. Bandrova, Proposal for a standard in cartographic visualization of natural risks and disasters, *Int. J. Unity Sci.* 10 (2) (2006) 130–139.
- [27] R.A. Bianchetti, J.O. Wallgrün, J.L. Yang, et al., Free classification of Canadian and American emergency management map symbol standards, *Cartogr. J.* 49 (4) (2012) 350–360.
- [28] A.C. Robinson, S. Pezanowski, S. Troedson, R. Bianchetti, J. Blanford, J. Stevens, E. Guidero, R.E. Roth, A.M. MacEachren, Symbol store: sharing map symbols for emergency management, *Cartogr. Geogr. Inf. Sci.* 40 (5) (2013), <https://doi.org/10.1080/15230406.2013.803833>.
- [29] D.A. Kuveždić, A. Dapo, B. Pribičević, Cartographic symbology for crisis mapping: a comparative study, *ISPRS Int. J. Geo-Inf.* 9 (3) (2020), 142.
- [30] U.J. Dymon, An analysis of emergency map symbology, *Int. J. Emerg. Manag.* 1 (3) (2003) 227–237.
- [31] S.B. Liu, L. Palen, The new cartographers: crisis map mashups and the emergence of neogeographic practice, *Cartogr. Geogr. Inf. Sci.* 37 (1) (2010) 69–90.
- [32] ANSI INCITS-415, *Homeland Security Mapping Standard—Point Symbology for Emergency Management*, American National Standard for Information Technology, Washington, DC, USA, 2006, 2006.
- [33] U.J. Dymon, E.K. Mbobi, Preparing an ANSI standard for emergency and hazard mapping symbology, in: *Proceedings of the 22nd International Cartographic Conference*. A Coruña, Spain: July 9–16, 2005.
- [34] Government of Canada's government operations centre: Canadian All-Hazards Symbology, Available online: <https://www.publicsafety.gc.ca>. (Accessed 5 December 2019).
- [35] Australian All Hazards Symbology, Emergency Management Spatial Information Australia, Version 2, 2018. Available online, <https://www.emsina.org/allhazardssymbolog>. (Accessed 5 December 2019).
- [36] Specification for emergency response plotting symbols; GB/T 35649-2017, Standardization Administration of the People's Republic of China: Beijing, China, 2017.
- [37] Q. Zhu, K.Z. Chen, X. Xie, et al., Site selection method of booster substations by integrating fuzzy analytic hierarchy process with 3D geographic information system, *J. Southwest Jiaot. Univ.* 54 (5) (2019) 980–988.
- [38] H.Y. Liu, X.P. Pang, Selection of Antarctic research stations based on GIS and fuzzy AHP, *Geomatics Inf. Sci. Wuhan Univ.* 40 (2) (2015) 249–252.
- [39] R. Likert, A technique for the measurement of attitudes, *Arch. Psychol.* 22 (140) (1932) 5–55.
- [40] H. Taherdoost, Determining sample size; how to calculate survey sample size, *Int. J. Econ. Manag. Syst.* 2 (2017) 237–239.
- [41] Y.J. Lü, Weight calculation method of fuzzy analytical hierarchy process, *Fuzzy Syst. Math.* (2) (2002) 79–85.
- [42] D.C. Ji, B.F. Song, T.X. Yu, FAHP and its application in the selection of design scheme, *Syst. Eng. Electron.* 28 (11) (2006), 1692–1552.
- [43] G. Lü, M. Chen, L. Yuan, L. Zhou, Y. Wen, M. Wu, B. Hu, Z. Yu, S.Y. Sheng, Y. Yue, Geographic scenario: a possible foundation for further development of virtual geographic environments, *Int. J. Digit. Earth* 11 (4) (2018) 356–368.

- [44] M. Chen, G. Lv, C. Zhou, H. Lin, Z. Ma, S. Yue, Y. Wen, F. Zhang, J. Wang, Z. Zhu, K. Xu, Geographic modeling and simulation systems for geographic research in the new era: Some thoughts on their development and construction, *Sci China Earth Sci* 64 (2021) 1207–1223.
- [45] L.Z. Yin, J. Zhu, Y. Li, et al., A virtual geographic environment for debris flow risk analysis in residential areas, *ISPRS Int. J. Geo-Inf.* 6 (11) (2017), 377.
- [46] R. Zhao, L. Zhan, M. Yao, L. Yang, A geographically weighted regression model augmented by Geodetector analysis and principal component analysis for the spatial distribution of PM_{2.5}, *Sustain. Cities Soc.* 56 (2020) 102106.
- [47] R. Zhao, M. Yao, L. Yang, H. Qi, X. Meng, F. Zhou, Using geographically weighted regression to predict the spatial distribution of frozen ground temperature: A case in the Qinghai-Tibet Plateau, *Environ. Res. Lett.* 16 (2) (2021), 024003.
- [48] L. Yang, Y. Ao, J. Ke, Y. Lu, Y. Liang, To walk or not to walk? Examining non-linear effects of streetscape greenery on walking propensity of older adults, *J. Transport Geogr.* 94 (2021) 103099.
- [49] G.L. Wang, Lessons learned from protective measures associated with the 2010 Zhouqu debris flow disaster in China, *Nat. Hazards* 69 (3) (2013) 1835–1847, <https://doi.org/10.1007/s11069-013-0772-1>.
- [50] Otani, et al., Effects of disaster management programs on individuals' preparedness in mount merapi, *J. Civil Eng. Forum* 4 (1) (2018) 79–90.